Nonlin. Processes Geophys. Discuss., https://doi.org/10.5194/npg-2017-67
Manuscript under review for journal Nonlin. Processes Geophys.
Discussion started: 12 February 2018

Nonlinear Processes in Geophysics
Discussions
Open Access
EGU

Stratified Kelvin-Helmholtz turbulence of compressible shear flows

Romit Maulik [1] and Omer San [1]

[1]School of Mechanical and Aerospace Engineering, Oklahoma State University, Stillwater, Oklahoma 74078

Correspondence to: Omer San (osan@okstate.edu)

Abstract. We study the scaling laws and structure functions of stratified shear flows by performing high-resolution numerical simulations of inviscid compressible turbulence induced by Kelvin-Helmholtz instability. An implicit large eddy simulation approach is adapted to solve our conservation laws for both two-dimensional (with a spatial resolution of $16,384^2$) and three-dimensional (with a spatial resolution of 512^3) configurations utilizing different compressibility characteristics such as shocks. For three-dimensional turbulence, we find that both kinetic energy and density-weighted energy spectra follow the classical Kolmogorov $k^{-5/3}$ inertial scaling. This phenomenon is observed due to the fact that the power density spectrum of three-dimensional turbulence yields the same $k^{-5/3}$ scaling. However, we demonstrate that there is a significant difference between these two spectra in two-dimensional turbulence since the power density spectrum flattens to $k^{-1/4}$. This flattening may be assumed to be a reason for the $k^{-7/3}$ scaling observed in the two-dimensional density-weight kinetic every spectra for high compressibility as compared to the k^{-3} scaling traditionally assumed with incompressible flows. Further inquiries are made to validate the statistical behavior of the various configurations studied through the use of second and third order velocity structure functions where it is noticed that scaling behavior differs between the two- and three-dimensional cases wherein only the latter is seen to follow trends from K41 theory.

1 Introduction

Turbulence is a highly nonlinear multiscale phenomenon which is ubiquitous in nature. It poses some of the most challenging problems in classical physics as well as in computational mathematics. Understanding the nature of compressible turbulence is of paramount importance. Highly compressible turbulence plays an important role in star formation control in dense molecular clouds (Padoan and Nordlund, 2002; Mac Low and Klessen, 2004; Mac Low et al., 1998) and are responsible for important design considerations in many engineering applications. Therefore, there have been several investigations into its statistical behavior. Kida and Orszag (1990) studied the mechanics of energy transfer and distribution as well as an examination of small-scale spectra in compressible turbulence with root-mean-square Mach numbers upto 0.9. Theoretical laws have also been advanced for the statistical behavior of turbulence quantities under the influence of compressibility effects (Shivamoggi, 1992; Lele, 1994; Shivamoggi, 2011; Wang et al., 2013). Kritsuk et al. (2007) utilized an adaptive mesh refinement (AMR) algorithm along with a piecewise parabolic approach for numerical dissipation to obtain scaling tendencies at high Mach number values for both kinetic energy, density weighted kinetic energy and density power spectra. In addition, structure functions of different orders were also studied and compared to the limiting case of incompressibility. Aluie (2013) provided a theoretical

Nonlin. Processes Geophys. Discuss., https://doi.org/10.5194/npg-2017-67
Manuscript under review for journal Nonlin. Processes Geophys.
Discussion started: 12 February 2018

justification of the presence of an inertial scale which is devoid of any effects of molecular viscosity for supersonic turbulence similar to the classical Richardson-Kolmogorov cascade in homogeneous isotropic incompressible turbulence (Kolmogorov, 1941; Vassilicos, 2015). Magnetic effects on the statistical behavior of supersonic turbulence have also been studied keenly due to implications for astrophysical processes such as in Banerjee and Galtier (2013) where two-point correlation function relations were studied. Scaling laws incorporating magnetic effects in hydrodynamic turbulence have also been proposed, for instance in Iroshnikov-Kraichnan theory (Iroshnikov, 1964; Kraichnan, 1965) where arguments similar to those used in Kolmogorov theory are used to explain statistical properties of small-scale components in velocity and magnetic fields. Extensions to account for the rather tenuous assumption of isotropy in compressible magnetohydrodynamics (MHD) have also been studied by Goldreich and Sridhar (1997). A generalization of the Iroshnikov-Kraichnan and Goldreich-Sridhar spectra to compressible magnetohydrodynamics has been presented by Shivamoggi (2008) where it is also shown to merge with the MHD shockwave spectrum in the limit of infinite compressibility (Kadomtsev and Petviashvili, 1973). A recent review which examines both hydrodynamic and magnetohydrodynamic implementations of supersonic compressible turbulence on statistical quantities can be found in Falceta-Goncalves et al. (2014). In this work, we follow the vast majority of investigations (Kuznetsov and Sereshchenko, 2015; Shivamoggi, 2015; Domaradzki and Carati, 2007; Sun, 2016; Westernacher-Schneider et al., 2015; Ottaviani, 1992; Qiu et al., 2016; Bershadskii, 2016) by utilizing the phenomenological description of turbulence in Fourier space as well as the utilization of two-point velocity structure functions for the statistical examination of our high fidelity numerical simulations. In terms of reference scaling behavior, we shall be comparing our numerical results against the theories advanced in Shivamoggi (1992) under the assumption of isentropic flow.

In this work, we shall examine the stratified compressible turbulence that emerges from a classical Kelvin-Helmholtz instability formulation. Similar problems have been studied extensively for their incompressible versions (Hopfinger, 1987; Werne and Fritts, 1999; Boffetta and Mazzino, 2017; Peltier and Caulfield, 2003). In this work, both two- and three-dimensional versions of stratification will be examined for their effects on scaling. It must be noted here that two-dimensional turbulence may be assumed to be an appropriate framework for many geophysical applications which exhibit extremely high aspect ratios and indeed, incompressible two-dimensional turbulence forms the cornerstone of geostrophic turbulence theory (Boffetta and Ecke, 2012; Shivamoggi, 1998). Astrophysical considerations have also been explored in Biskamp and Schwarz (2001) where the effects of a magnetohydrodynamic coupling have also been examined on scaling behavior. Our focus shall primarily rest on a comparison of numerically obtained behavior of the density power spectrum, the averaged kinetic energy spectrum and the density weighted kinetic energy spectrum along with second and third order velocity structure functions with their theoretical predictions. Some reference scaling laws (in the incompressible limit) we shall be using for comparison are the classical Kolmogorov scaling (Kolmogorov, 1941) for isotropic three-dimensional turbulence and Kraichnan scaling (Kraichnan, 1967) for two-dimensional isotropic turbulence.

A common strategy for the numerical examination of the statistics of highly compressible turbulence is the use of the Eulerian hydrodynamic conservation laws implemented through an implicit large eddy simulation (ILES) methodology (Passot et al., 1988; Blaisdell et al., 1993). This is because it is commonly accepted that an ILES formulation of the Euler equations provides a good estimation for the Navier-Stokes equations in the limit of infinite Reynolds numbers (Bos and Bertoglio, 2006; Zhou et al.,

Nonlin. Processes Geophys. Discuss., https://doi.org/10.5194/npg-2017-67
Manuscript under review for journal Nonlin. Processes Geophys.
Discussion started: 12 February 2018

Nonlinear Processes in Geophysics
Discussions
Open Access
EGU

2014; Sytine et al., 2000). However, two conditions must be enforced in order to satisfy the aforementioned assumption. Firstly, vorticity must be introduced via either boundary and/or initial conditions since the Euler equations are incapable of generating vorticity from irrotational flows. Secondly, an artificial viscosity must be incorporated into the simulation mechanism to mimic the preservation of dissipative behavior of the Navier-Stokes equations in the inviscid limit (Moura et al., 2017). The ILES mechanism is a suitable approach for artificial dissipation through the use of numerical truncation errors and is our simulation algorithm of choice for the high fidelity numerical experiments in this investigation.

The question we attempt to address through this work is related to the difference between purely averaged kinetic energy spectra scaling and density weighted spectra scaling for both two- and three-dimensional compressible turbulence. Our observations suggest a different 'packaging' of density in the spectral space for the two-dimensional turbulence case. This is proven conclusively by comparing the differences in density power spectrum behavior for both two- and three-dimensional configurations. It is proposed that the density power spectrum (or in other words the packaging of density at different wavenumbers) may be a reason that causes a variation in the k^{-3} scaling of the density-weighted kinetic energy cascade with changing compressibility (higher compressibilities are observed to show $k^{-7/3}$ scaling) for two-dimensional turbulence as against the constant $k^{-5/3}$ cascade in three-dimensional turbulence. Our results are also validated through the use of second and third order structure function behavior with varying compressibility. High fidelity simulation data are generated by utilizing 512^3 and 16384^2 degrees of freedom for the three- and two-dimensional cases respectively. We demonstrated that there is no difference in energy spectrum scalings between kinematic and density weighted velocities in three-dimensional simulations since both the power density and velocity spectra scale with the $k^{-5/3}$. However, we have demonstrated that the difference becomes pronounced in two-dimensional simulations because power density spectrum scales with $k^{-1/4}$. Ultimately, it is our aim to link these analyses to nonlinear processes exhibiting very high aspect ratios for astrophysical, heliophysical and plasma physics applications.

2 Compressible turbulence

The governing laws utilized for our numerical experiments are given by the Euler equations which may be expressed in their dimensionless differential form as

$$\frac{\partial \rho}{\partial t} + \nabla.(\rho \boldsymbol{u}) = 0 \tag{1}$$

$$\frac{\partial (\rho \boldsymbol{u})}{\partial t} + \nabla.(\rho \boldsymbol{u} \otimes \boldsymbol{u} + p\boldsymbol{I}) = 0 \tag{2}$$

$$\frac{\partial (\rho E)}{\partial t} + \nabla.(\rho E \boldsymbol{u} + p\boldsymbol{u}) = 0 \tag{3}$$

where ρ is the fluid density, $\boldsymbol{u} = \{u, v\}^T \in \mathbb{R}^2$ and $\boldsymbol{u} = \{u, v, w\}^T \in \mathbb{R}^3$ is the flow velocity in a Cartesian co-ordinate system, p is the static pressure, and E is the total energy per unit mass. Assuming a perfect gas with a ratio of specific heats γ, the

Nonlin. Processes Geophys. Discuss., https://doi.org/10.5194/npg-2017-67
Manuscript under review for journal Nonlin. Processes Geophys.
Discussion started: 12 February 2018

pressure can be determined by an equation of state which closes our coupled governing equations given by

$$p = \rho(\gamma - 1)\left(E - \frac{1}{2}(\boldsymbol{u}.\boldsymbol{u})\right) \tag{4}$$

where we have set $\gamma = 7/5$ in our study. Note that the assumption of the classical equation of state for relating the pressure and total energy of the flow ensures the interaction of solely acoustic and vortical modes (Shivamoggi, 1992). Our computational domain also exhibits periodic boundary conditions in all directions.

2.1 Stratified Kelvin-Helmholtz instability

The stratified Kelvin-Helmholtz instability (KHI) test-case is a famous problem which manifests itself when there is a velocity difference at the interface between two fluids of different densities (Thomson, 1871). It can commonly be observed through experimental observation, numerical simulation and it is also visible in many natural phenomena such as for example in situations with wind flow over bodies of water causing wave formation and in the planet Jupiter's atmosphere between atmospheric bands moving at different speeds (Hwang et al., 2012). The study of this instability in a benchmark formulation reveals key information about the transition to turbulence for two fluids moving at different speeds. For these practical applications, it is common to choose a double shear layer problem to simulate the formation of KHI in a periodic two-dimensional computational setting with unit side length. This stratified shear layer instability problem is used to demonstrate the evolution of linear perturbations into a transition to nonlinear two-dimensional hydrodynamic turbulence. The instability triggers small-scale vortical structures at the sharp density interface initially which eventually transitions through nonlinear interactions to a completely turbulent field.

2.2 Two-dimensional simulations

A two-dimensional implementation of the dual-shear layer KHI problem is devised through our aforementioned unstable perturbed compressible shear layer. This may be implemented through our computational domain which is a square of unit side length with the following initial conditions

$$\rho(x,y) = \begin{cases} 1.0, & \text{if } |y| \geq 0.25 \\ 2.0, & \text{if } |y| < 0.25 \end{cases} \tag{5}$$

$$u(x,y) = \begin{cases} \alpha, & \text{if } |y| \geq 0.25 \\ -\alpha, & \text{if } |y| < 0.25 \end{cases} \tag{6}$$

$$v(x,y) = \lambda \sin(2\pi n x/L) \tag{7}$$

$$p(x,y) = 2.5. \tag{8}$$

We can observe that the vertical component of the velocity is perturbed using a single-mode sine wave ($n = 2, L = 1$) with an amplitude $\lambda = 0.01$. Our two-dimensional numerical experiments are solved to a final dimensionless time of $t = 5$. We

Nonlin. Processes Geophys. Discuss., https://doi.org/10.5194/npg-2017-67
Manuscript under review for journal Nonlin. Processes Geophys.
Discussion started: 12 February 2018

clarify that the $\mathbb{R}^2$ simulation domain for all experiments is set in $(x, y) \in [-0.5, 0.5] \times [-0.5, 0.5]$ with $N^2 = 16,384^2$ degrees of freedom. Fig. (1) represents a schematic expressing the initial conditions of our two-dimensional simulation. We remark, that in this study we perform implicit large eddy simulation (ILES) simulations by using a finite volume framework. Our numerical scheme utilizes the fifth-order weighted essential non-oscillatory (WENO) reconstructions equipped with the Roe's approximate Riemann solver (Roe, 1981) at the cell interfaces. It is well-known that the utilization of artificial dissipation of ILES schemes(from the numerical viscosity of biased state reconstructions) mimics the physical viscosity of the Navier-Stokes equations in the limit of infinite Reynolds numbers. We utilize a parallel approach for the computational solution of our governing laws implemented in the OpenMPI framework. Details about implementation and the computational performance of our solver may be found in Maulik and San (2017) additionally showing weak and strong scaling tests. Our three-dimensional simulations employ a similar approach.

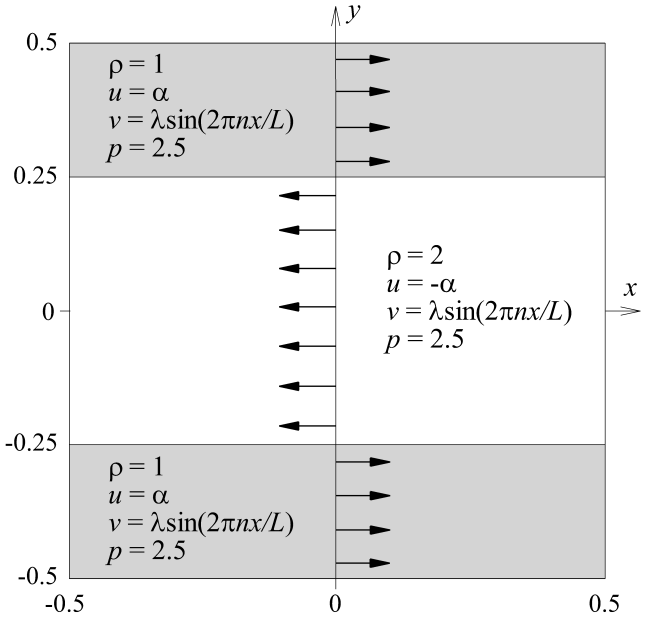

Figure 1. Stratified Kelvin-Helmholtz instability problem in a periodic square box of side length $L = 1$. Our initial condition reads a single-mode perturbation to the y-component of the velocity to trigger the instability with $n = 2$ and the amplitude $\lambda = 0.01$. We extend this 2D domain along z-direction to perform our 3D simulations in a triple periodic domain with size of L in each side where we also use an initial perturbation to the z-component of the velocity given by $w = \lambda \sin(2\pi n z/L)$.

Fig. (2) describes snapshots in time of the density field for this two-dimensional compressible turbulence test case when $\alpha = 1.0$. One can notice a transition to turbulence once an initial instability has developed. The shearing velocity magnitude given by α controls the compressibility which is apparent from comparisons with Figs. 3 and 4 where smaller values lead to formation of much smoother structures and consequently lead to shock-free fields towards to the limit of incompressibility. Evidence from

Nonlin. Processes Geophys. Discuss., https://doi.org/10.5194/npg-2017-67
Manuscript under review for journal Nonlin. Processes Geophys.
Discussion started: 12 February 2018

Fig. (4) also shows a delay in the onset of turbulence due to a reduced shearing velocity. Table 1 also demonstrates the mean and maximum Mach number values at the final computational time $t = 5$. It is clear that the case for $\alpha = 0.25$ corresponds to perfectly subsonic regime with lower compressibility (i.e., the mean Mach number of $M = 0.15$).

Table 1. The mean and maximum Mach numbers computed at final time $t = 5$.

Resolution	α	$M^{t=5}_{mean}$	$M^{t=5}_{max}$
$16,384^2$	1.0	0.55	1.40
$16,384^2$	0.5	0.30	1.28
$16,384^2$	0.25	0.15	0.73

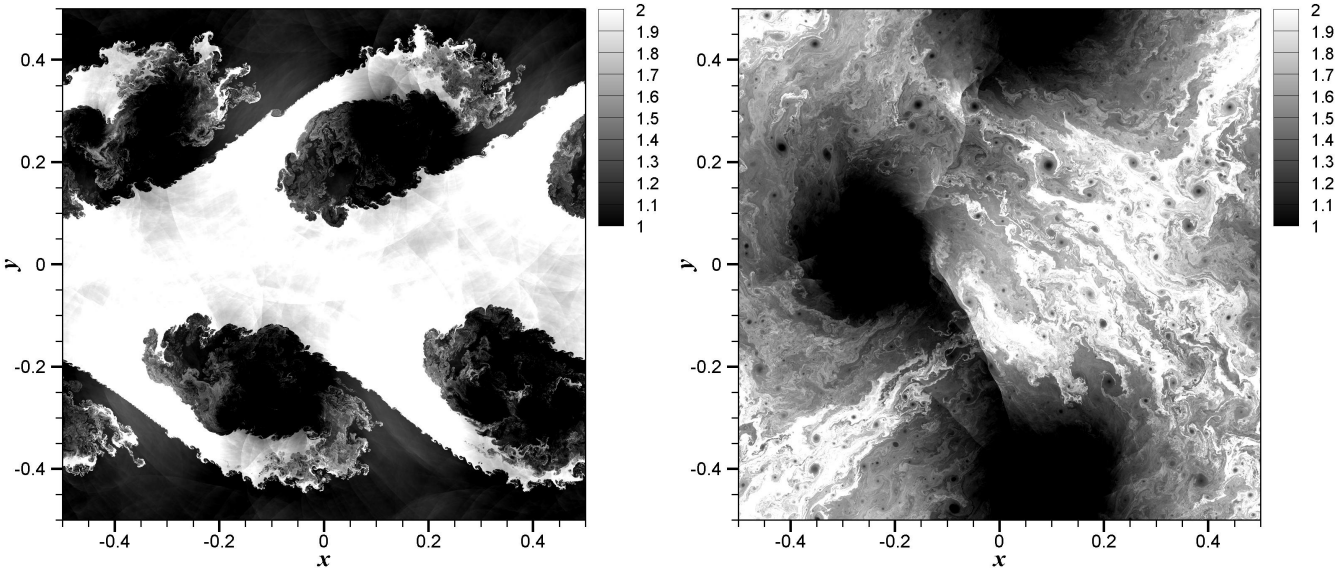

Figure 2. Time evolution of density field the 2D KHI turbulence with $\alpha = 1.0$ demonstrating results at $t = 1$ (left) and $t = 5$ (right) obtained by a grid resolution of $N^2 = 16,384^2$.

2.3 Three-dimensional simulations

While two-dimensional compressible turbulence investigations are valuable for insight into the physical processes of systems which exhibit extreme aspect ratios (Boffetta and Ecke, 2012), it is well known that the process of energy transfer between scales is fundamentally different when compared to that of three-dimensional flows (Clercx and van Heijst, 2017). Isotropic, homogeneous, incompressible 3D-turbulence is characterized by the famous Kolmogorov-Richardson cascade of energy where the largest vortices continuously inject energy into an inertial cascade which terminates in the Kolmogorov length scale (Kol-

Nonlin. Processes Geophys. Discuss., https://doi.org/10.5194/npg-2017-67
Manuscript under review for journal Nonlin. Processes Geophys.
Discussion started: 12 February 2018

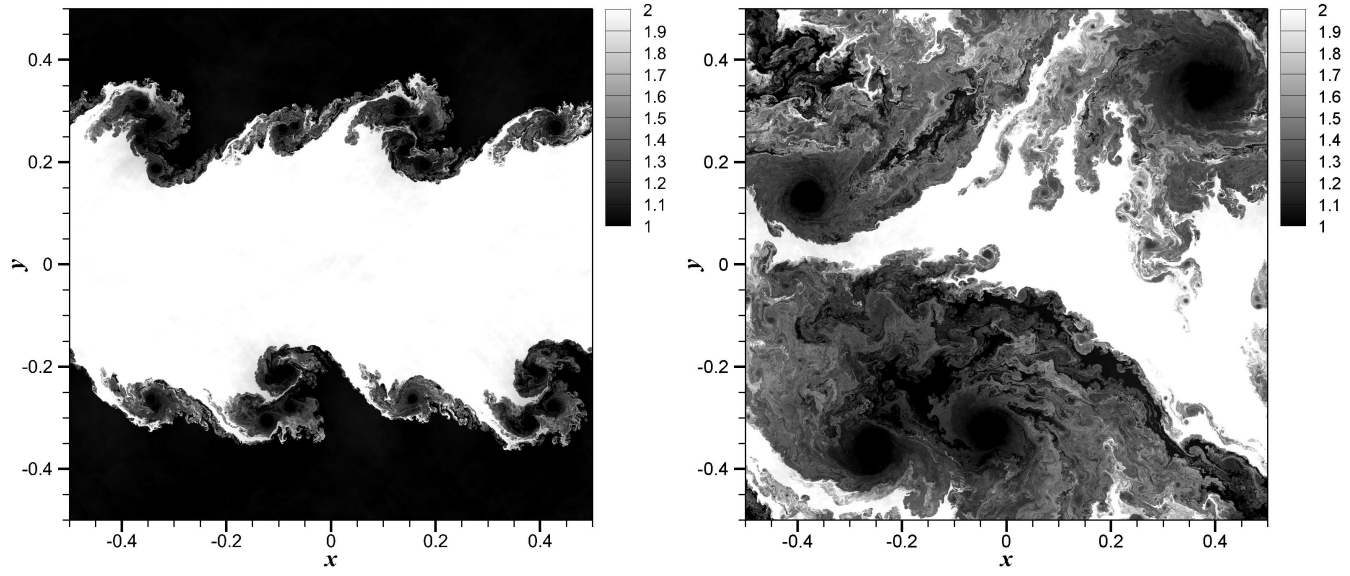

Figure 3. Time evolution of density field the 2D KHI turbulence with $\alpha = 0.5$ demonstrating results at $t = 1$ (left) and $t = 5$ (right) obtained by a grid resolution of $N^2 = 16,384^2$.

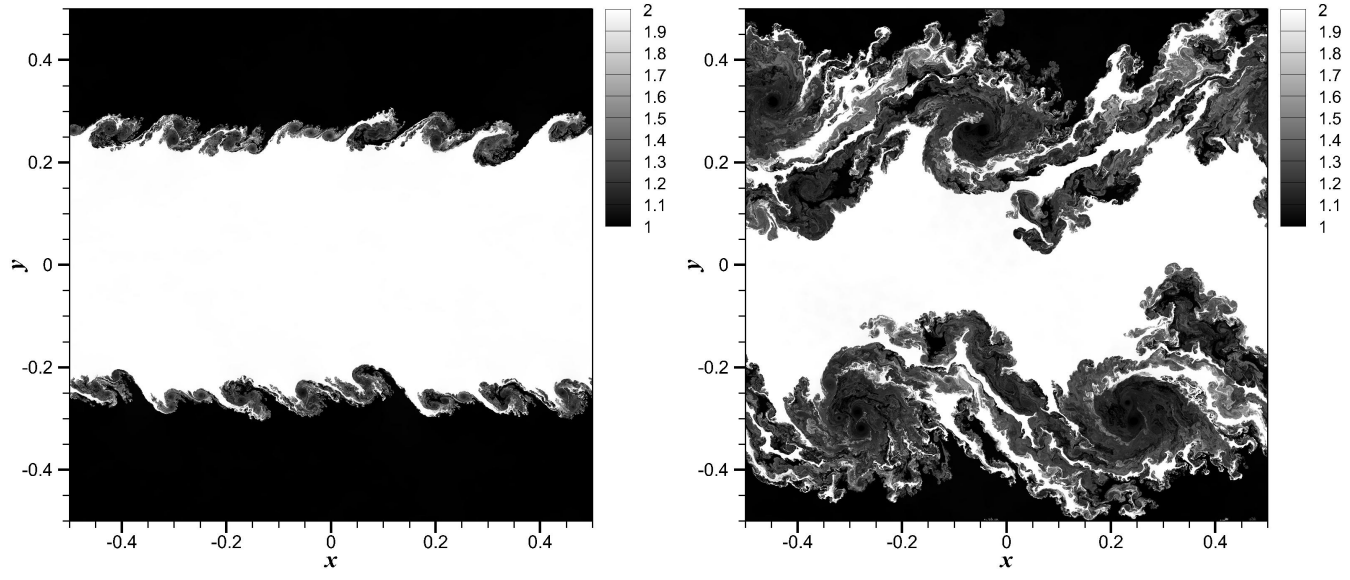

Figure 4. Time evolution of density field the 2D KHI turbulence with $\alpha = 0.25$ demonstrating results at $t = 1$ (left) and $t = 5$ (right) obtained by a grid resolution of $N^2 = 16,384^2$.

Nonlin. Processes Geophys. Discuss., https://doi.org/10.5194/npg-2017-67
Manuscript under review for journal Nonlin. Processes Geophys.
Discussion started: 12 February 2018

mogorov, 1941) where viscous effects dissipate this energy. This is particularly applicable for engineering flows where it has been established that turbulence 'decays' in the absence of forcing due to viscous dissipation. In contrast, two-dimensional turbulence exhibits the presence of an inverse energy cascade (given by Kraichnan-Bachelor-Leith theories (Kraichnan, 1967; Leith, 1971; Batchelor, 1969)) where energy from the smallest scales is transferred to largest scales. This has implications for the restoration of local isotropy (since large scale structures created by the inverse energy cascade affect the amount of enstrophy in the field and thus affect the energy dissipation rate). In the presence of a-periodic boundary conditions (a subject of future investigations), these newly created large scale structures may lead to significant alteration in scaling laws. In essence, we also simulate high-fidelity three-dimensional compressible turbulence data to contrast the statistical behavior of turbulence in two and three dimensions.

Our computational domain for the three-dimensional turbulence case is analogous to that of the two-dimensional domain. We utilize a domain given by a $\mathbb{R}^3$ set in $(x, y, z) \in [-0.5, 0.5] \times [-0.5, 0.5] \times [-0.5, 0.5]$ with $N^3 = 512^3$ degrees of freedom. Our initial conditions are given by

$$\rho(x,y,z) = \begin{cases} 1.0, & \text{if } |y| \geq 0.25 \\ 2.0, & \text{if } |y| < 0.25 \end{cases} \tag{9}$$

$$u(x,y,z) = \begin{cases} \alpha, & \text{if } |y| \geq 0.25 \\ -\alpha, & \text{if } |y| < 0.25 \end{cases} \tag{10}$$

$$v(x,y,z) = \lambda \sin(2\pi n x/L) \tag{11}$$

$$w(x,y,z) = \lambda \sin(2\pi n z/L) \tag{12}$$

$$p(x,y,z) = 2.5. \tag{13}$$

and periodic boundary conditions in all directions. We keep our parameters n, L and λ similar to those used in the two-dimensional case and utilize $N^3 = 512^3$ degrees of freedom for the simulation of our computational domain.

Fig. (5) shows the density field at times $t = 1$ and $t = 5$ for a shearing velocity magnitude of $\alpha = 1.0$. One can observe how the solution domain has transitioned almost entirely to a turbulent field for this case as against the very visible stratification observed in lower compressibility simulations given by $\alpha = 0.5$ and $\alpha = 0.25$ shown in Figs. (6) and (7) respectively. Our aim is to quantify the effect of the shearing velocity on the compressibility and scaling laws of these two- and three-dimensional configurations.

Nonlin. Processes Geophys. Discuss., https://doi.org/10.5194/npg-2017-67
Manuscript under review for journal Nonlin. Processes Geophys.
Discussion started: 12 February 2018

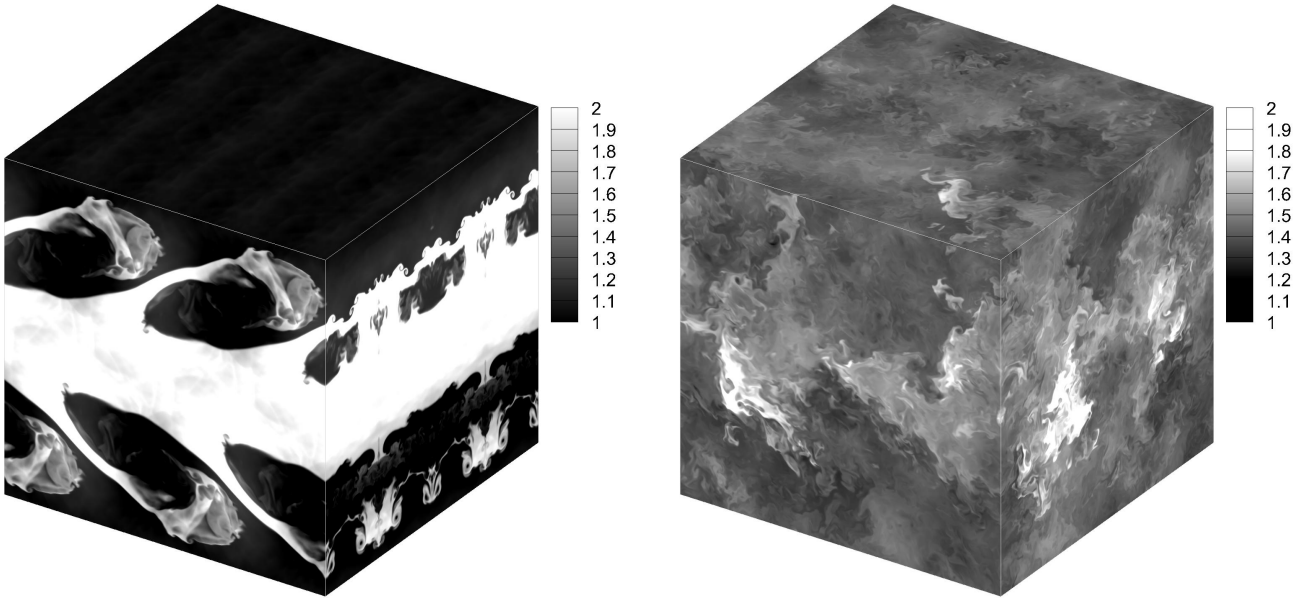

Figure 5. Time evolution of density field for the 3D KHI turbulence with $\alpha = 1.0$ demonstrating results at $t = 1$ (left) and $t = 5$ (right) obtained by a grid resolution of $N^3 = 512^3$.

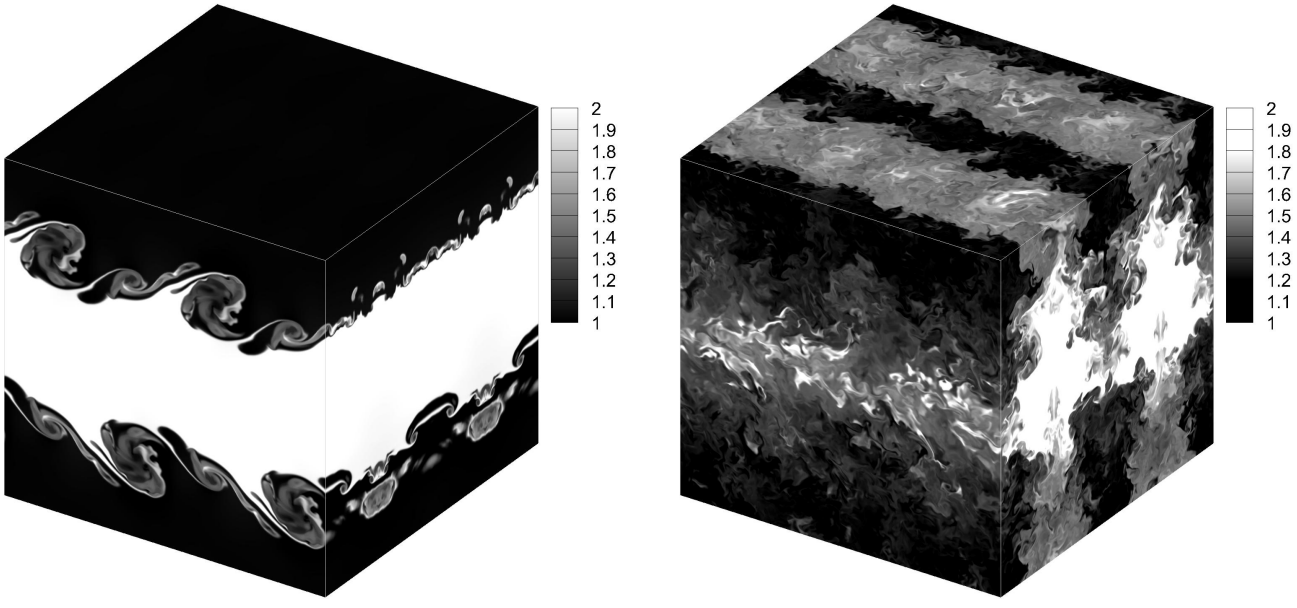

Figure 6. Time evolution of density field for the 3D KHI turbulence with $\alpha = 0.5$ demonstrating results at $t = 1$ (left) and $t = 5$ (right) obtained by a grid resolution of $N^3 = 512^3$.

Nonlin. Processes Geophys. Discuss., https://doi.org/10.5194/npg-2017-67
Manuscript under review for journal Nonlin. Processes Geophys.
Discussion started: 12 February 2018

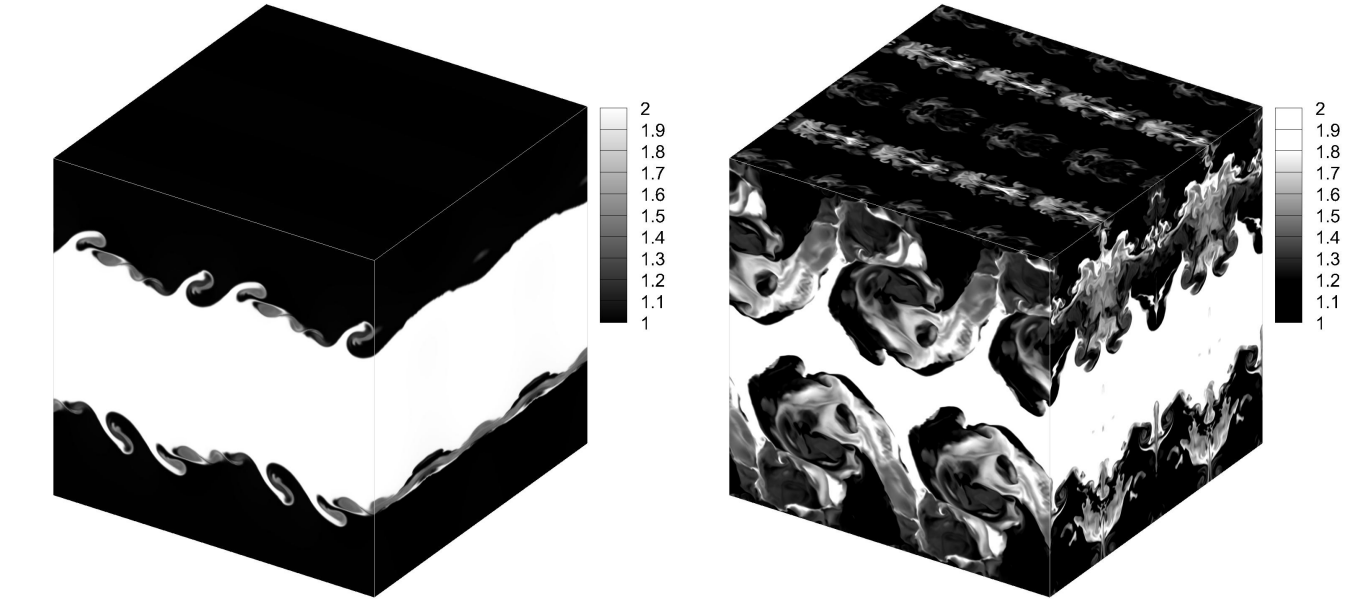

Figure 7. Time evolution of density field for the 3D KHI turbulence with $\alpha = 0.25$ demonstrating results at $t = 1$ (left) and $t = 5$ (right) obtained by a grid resolution of $N^3 = 512^3$.

3 Turbulence statistics and scaling exponents

3.1 Kinetic energy spectrum

The first statistical measure we investigate is given by the classical kinetic energy spectra which may be calculated using the following expression in wavenumber space (Kida et al., 1990)

$$\hat{E}(\mathbf{k},t) = \frac{1}{2}|\hat{\mathbf{u}}(\mathbf{k},t)|^2 \tag{14}$$

where $\hat{\mathbf{u}}(\mathbf{k},t)$ is the Fourier transform of the velocity vector in the wavenumber space. Eq. (14) can be also rewritten in terms of velocity components (assuming a two-dimensional Cartesian domain) as

$$\hat{E}(\mathbf{k},t) = \frac{1}{2}\left(|\hat{u}(\mathbf{k},t)|^2 + |\hat{v}(\mathbf{k},t)|^2\right) \tag{15}$$

where we compute velocity components $\hat{u}(\mathbf{k},t)$ and $\hat{v}(\mathbf{k},t)$ using a fast Fourier transform algorithm **?**. Finally, the spectra can be calculated by angle averaging in the following manner

$$E(k,t) = \sum_{k-\frac{1}{2}\leq|\acute{\mathbf{k}}|<k+\frac{1}{2}} \hat{E}(\acute{\mathbf{k}},t) \tag{16}$$

where $k = |\mathbf{k}| = \sqrt{k_x^2 + k_y^2}$ in $\mathbb{R}^2$. Extensions to three-dimensions are straightforward.

Nonlin. Processes Geophys. Discuss., https://doi.org/10.5194/npg-2017-67
Manuscript under review for journal Nonlin. Processes Geophys.
Discussion started: 12 February 2018

Nonlinear Processes in Geophysics
Discussions
Open Access
EGU

3.2 Density-weighted kinetic energy spectrum

The kinetic energy spectrum is generally utilized for characterizing the energy content of scales in incompressible turbulent flows and as such do not take into consideration, the localized scale content of the density. To include these density effects, following Lele (1994); Kritsuk et al. (2007), we define an energy spectrum built on density-weighted velocity $\boldsymbol{\omega} = \sqrt{\rho}\boldsymbol{u}$ i.e.

$$\hat{E}(\mathbf{k}, t) = \frac{1}{2}|\hat{\boldsymbol{\omega}}(\mathbf{k}, t)|^2 \tag{17}$$

Fig. (8) describes the spherical averaged energy spectra for the three-dimensional test case. Note here that the spherical average implies that the local energy content in the Fourier domain is integrated over a spherical shell of radius k in three dimensions. One can observe a scaling behavior that corresponds to classical Kolmogorov theory in the infinite Reynolds number limit (i.e. an inertial range with $k^{-5/3}$ scaling) for both purely kinetic energy spectra and density-weighted kinetic energy spectra. The finer dissipative scales are seen to display a k^{-6} scaling behavior for both these statistical quantities as well. Although, not conclusive, a comparison with $k^{-15/8}$ may suggest close agreement with Shivamoggi (1992) where this behavior is expected for weak random sound fields (a byproduct of low compressibility). For an analogy with the two-dimensional test cases, we present a transversely-averaged energy spectra in Fig. (9) wherein the circular averaging of the energy in the Fourier domain is carried out over different two-dimensional z planes which are then ensemble averaged over the depth of the domain. Similar trends to the spherical averaging spectral scaling are observed for this case.

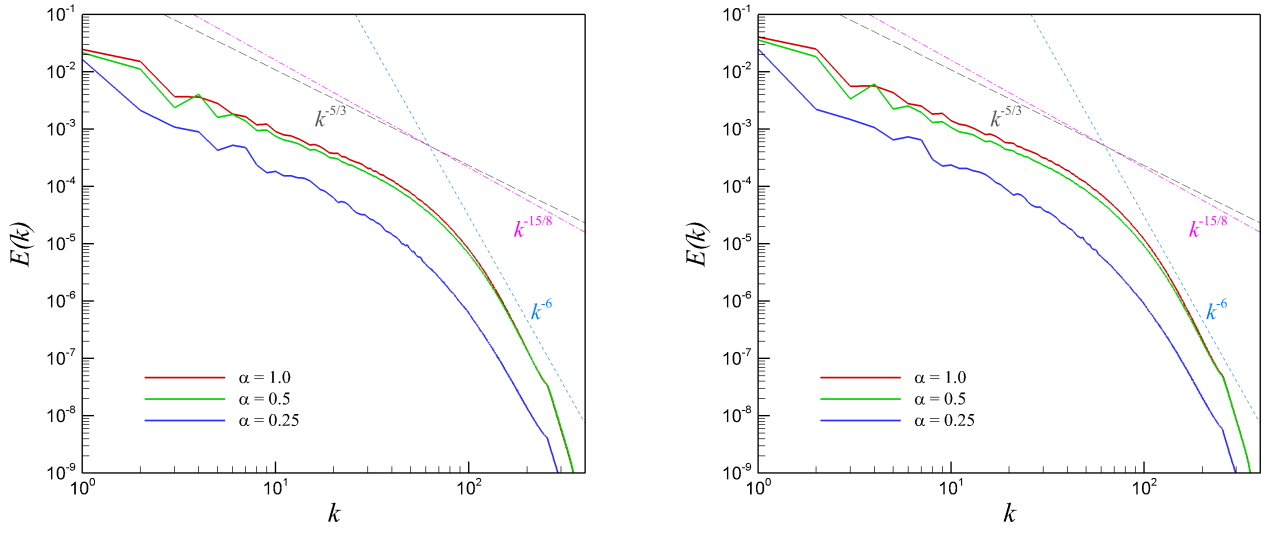

Figure 8. Spherical-averaged energy spectra for the 3D KHI turbulence. Left: spectra built on using the kinetic velocity $\boldsymbol{u}$. Right: spectra built on using the density-weighted velocity $\boldsymbol{\omega} = \sqrt{\rho}\boldsymbol{u}$.

Nonlin. Processes Geophys. Discuss., https://doi.org/10.5194/npg-2017-67
Manuscript under review for journal Nonlin. Processes Geophys.
Discussion started: 12 February 2018

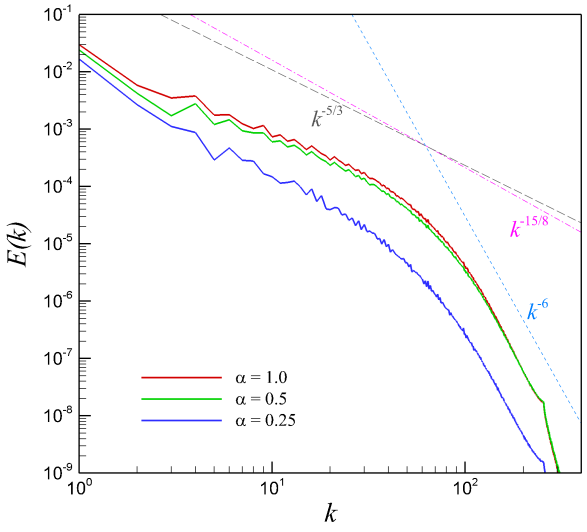

Figure 9. Transversely-averaged energy spectra for the 3D KHI turbulence. An angle-averaged kinetic energy spectrum is first computed at each z-plane and then followed by an ensemble averaging procedure along the z-direction.

We investigate the performance of the same metrics for the two-dimensional test case and obtain scaling behavior as seen in Fig. (10) where a k^{-3} scaling behavior is obtained in accordance with the inverse-energy cascade espoused by Kraichnan-Batchelor-Leith theory for the inertial range. A higher magnitude of α is seen to delay the formation of the k^{-6} cascade in the dissipation range. Fig. (10) also shows the spectral scaling obtained from the density-weighted kinetic energy spectra where scaling behavior corresponding to $k^{-7/3}$ is seen. This suggests that the two-dimensional configuration of the test-case is affected by the packaging of density content at different scales. The dissipation zone shows a similar behavior using this metric where a delay in scaling with k^{-6} is obtained by an increase in the magnitude of α. Fig. (11) shows the effect of the parameter α on the compressibility of the two-dimensional turbulence case through the use of a compensated energy spectra where the distance from the origin in the Fourier space (in other words k) is used to weight instantaneous energy content (i.e. $E(\mathbf{k})$). At $\alpha = 1.0$ one can observe a distinct loss of isotropy in the energy content of the solution field (in spectral space) which corresponds to an enhanced compressibility. In comparison, $\alpha = 0.5$ and $\alpha = 0.25$ display a behavior which is rather isotropic in nature indicating weak compressibility.

3.3 Density power spectrum

In order to solely quantify the effect of the scale content of density, we devise a power spectrum that reflects the average packaging of density over different scales at any given time in the simulation. This may be given by the following expression

$$\hat{P}(\mathbf{k},t) = \frac{1}{2}|\hat{\rho}(\mathbf{k},t)|^2, \tag{18}$$

Nonlin. Processes Geophys. Discuss., https://doi.org/10.5194/npg-2017-67
Manuscript under review for journal Nonlin. Processes Geophys.
Discussion started: 12 February 2018

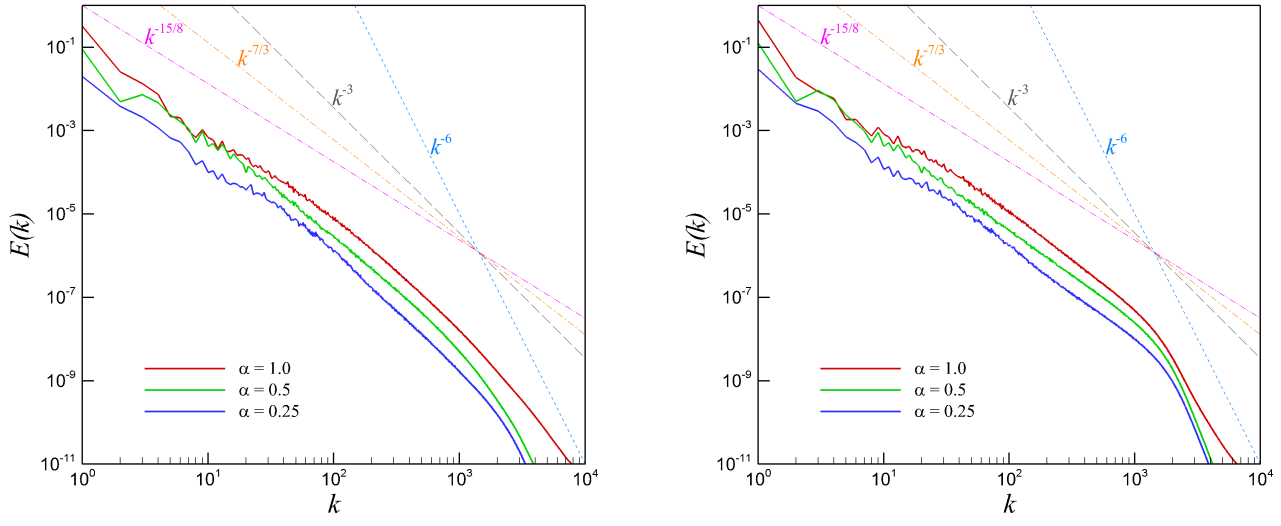

Figure 10. Angle-averaged energy spectra for the 2D KHI turbulence. Left: spectra built on using the kinetic velocity $\boldsymbol{u}$. Right: spectra built on using the density-weighted velocity $\boldsymbol{\omega} = \sqrt{\rho}\boldsymbol{u}$.

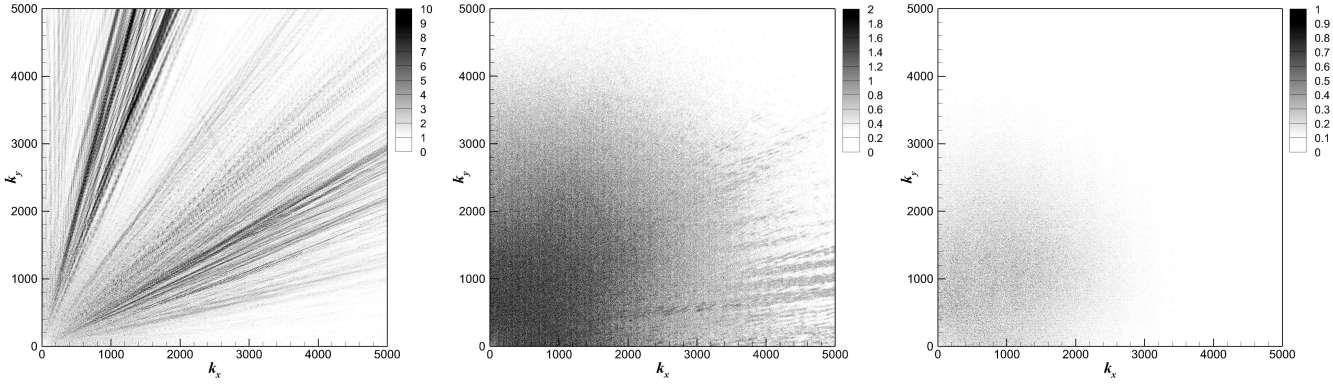

(a) $\alpha = 1.0$ (b) $\alpha = 0.5$ (c) $\alpha = 0.25$

Figure 11. Compensated, $k^4\hat{E}(\mathbf{k}, t = 5)$, kinetic energy spectra for the 2D KHI turbulence for various α values.

Nonlin. Processes Geophys. Discuss., https://doi.org/10.5194/npg-2017-67
Manuscript under review for journal Nonlin. Processes Geophys.
Discussion started: 12 February 2018

followed by angle averaging which leads to

$$P(k,t) = \sum_{k-\frac{1}{2}\leq|\acute{\mathbf{k}}|<k+\frac{1}{2}} \hat{P}(\acute{\mathbf{k}},t). \tag{19}$$

The observations regarding the difference in scaling behavior of the kinetic energy and density-weighted kinetic energy spectra give us a cause to compare the scaling behavior of the density power spectra for both of our two- and three-dimensional test cases. Fig. (12) shows the density power spectra for the three-dimensional turbulence test case where it can be seen that a five-thirds law is followed for the arrangement of density content in the solution field. A dissipation range scaling of k^{-6} can also be observed. It can be seen that the variation of parameter α does not seem to affect scaling behavior appreciably. Fig. (14) shows a similar examination for the two-dimensional test case where a considerable difference in scaling behavior is observed. The imposition of two-dimensional turbulence leads to a considerable alteration in the scaling behavior of the density power spectrum with a $k^{-1/4}$ scaling observed in the inertial range and a k^{-3} scaling in the dissipation range. In fact, this packaging of density consequently affects the density-weighted kinetic energy spectra described in Fig. (10). The intercomparison of the two- and three-dimensional statistical quantities suggests that the density power spectrum (i.e. the arrangement of density at different wavenumbers) plays an important role with increased compressibility of any simulation wherein the $k^{-1/4}$ scaling causes a deviation from k^{-3} scaling associated with two-dimensional incompressibility to $k^{-7/3}$ scaling for $\alpha = 1.0$ for the same test-case. In contrast, the $k^{-5/3}$ density power spectrum of three-dimensional turbulence causes no variation in scaling behavior with increased compressibility and also causes similar scaling behaviors for both averaged kinetic energy spectra as well as averaged density-weighted kinetic energy spectra as seen in Fig. (8). This is a central conclusion of this investigation.

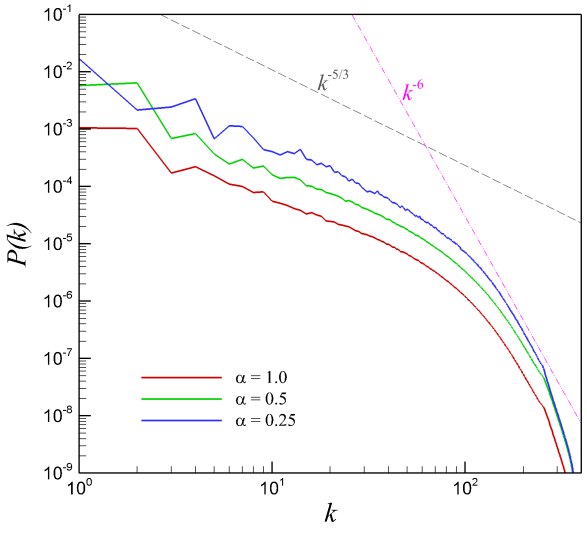

Figure 12. Spherical-averaged density power spectra for the 3D KHI turbulence.

Nonlin. Processes Geophys. Discuss., https://doi.org/10.5194/npg-2017-67
Manuscript under review for journal Nonlin. Processes Geophys.
Discussion started: 12 February 2018

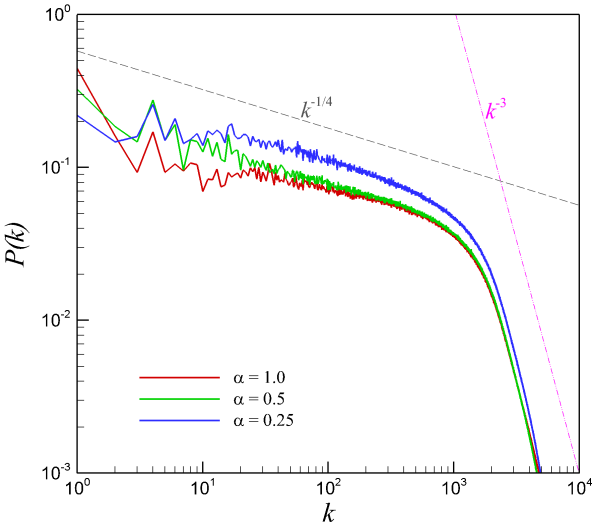

Figure 13. Angle-averaged density power spectra for the 2D KHI turbulence.

3.4 Velocity structure functions

Statistical inferences about the nature of compressible turbulence may also be drawn through the use of velocity structure functions which also show scaling tendencies according to the physics of the solution field Moin and Yaglom (1975). A velocity structure function may be expressed as Boffetta and Ecke (2012)

$$S^p(r) = \langle |\boldsymbol{u}(\boldsymbol{x}+\boldsymbol{x}) - \boldsymbol{u}(\boldsymbol{r})|^p \rangle \tag{20}$$

where the ensemble averaging is taken over all positions $\boldsymbol{x}$ and all orientations of $\boldsymbol{r}$ within the computational domain to yield statistics for the length scale $r = |\boldsymbol{r}|$. Our choice of p determines the *order* of the structure function we are examining and this investigation looks at $p = 2$ and $p = 3$ for the characterization of turbulence in both two and three dimensions. Both longitudinal ($\boldsymbol{u} \parallel \boldsymbol{r}$) and transverse ($\boldsymbol{u} \perp \boldsymbol{r}$) third-order velocity structure functions are computed. In our assessments, a range of $10^{-2} \leq r \leq 10^{-1}$ is assumed to represent the general vicinity of the inertial range.

We utilize the high fidelity data of the previously described numerical experiments for two- and three-dimensional turbulence to obtain structure function statistics at time $t = 5$. Fig. (14) shows the second-order velocity structure function for the longitudinal and transverse directions for the 3D test case. One can observe a steadily increasing alignment with $r^{2/3}$ with decreasing value of α implying weaker compressibility. It is worthy to mention here that K41 theory dictates a cascade given by $p/3$. Similar trends are observed for both longitudinal and transverse directions suggesting that a certain degree of isotropy now characterizes the system. Fig. (15) shows the third-order structure functions where we once again see that the scaling tendencies follow r^1 with decreasing α for both longitudinal and transverse directions. For ranges of r below 10^{-2}, it is observed

Nonlin. Processes Geophys. Discuss., https://doi.org/10.5194/npg-2017-67
Manuscript under review for journal Nonlin. Processes Geophys.
Discussion started: 12 February 2018

Nonlinear Processes in Geophysics
Discussions
Open Access
EGU

that both longitudinal and transverse structure functions scale according to r^2 for the second-order structure function and r^3 for the third-order structure function.

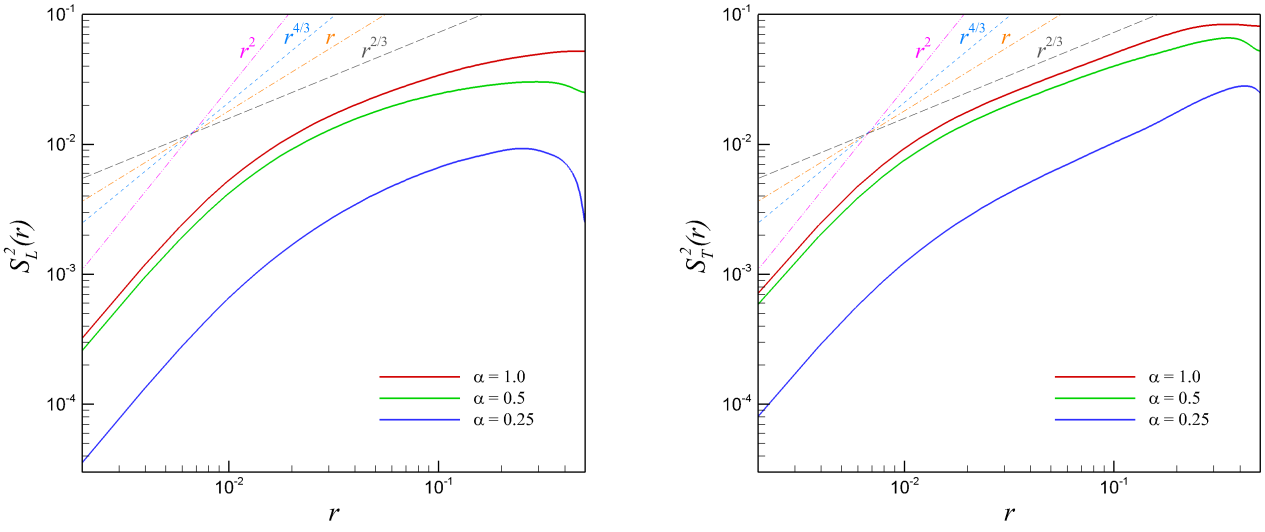

Figure 14. Second-order velocity structure functions for the 3D KHI turbulence. Left: longitudinal ($\boldsymbol{u} \parallel \boldsymbol{r}$). Right: transverse ($\boldsymbol{u} \perp \boldsymbol{r}$).

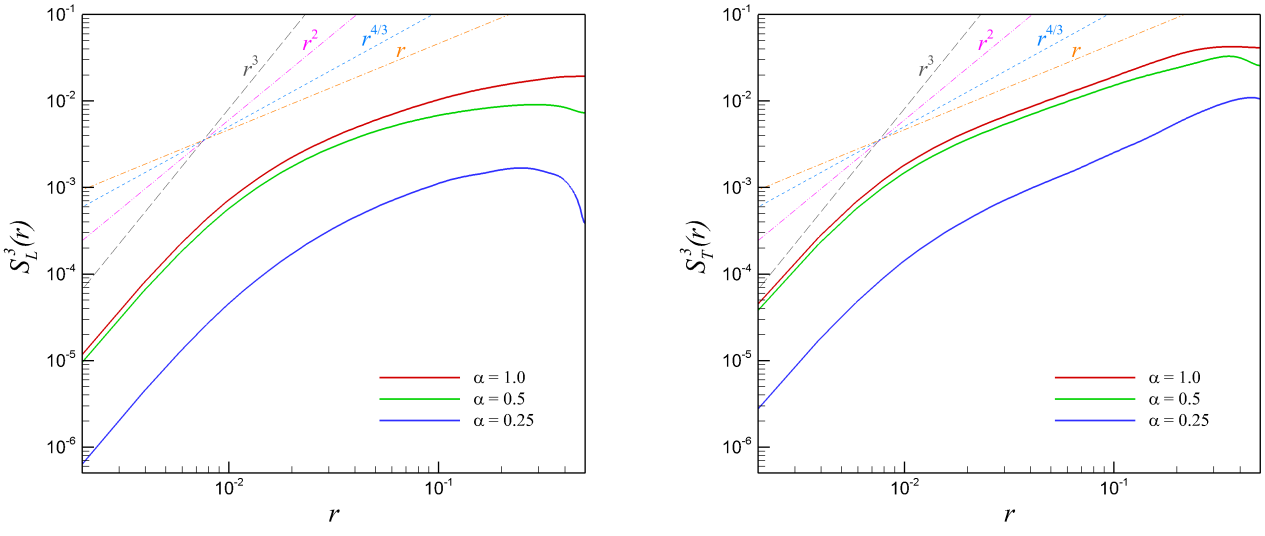

Figure 15. Third-order velocity structure functions for the 3D KHI turbulence. Left: longitudinal ($\boldsymbol{u} \parallel \boldsymbol{r}$). Right: transverse ($\boldsymbol{u} \perp \boldsymbol{r}$).

Nonlin. Processes Geophys. Discuss., https://doi.org/10.5194/npg-2017-67
Manuscript under review for journal Nonlin. Processes Geophys.
Discussion started: 12 February 2018

We undertake a similar statistical examination for our two-dimensional test case where second-order longitudinal and transverse structure functions are given by Fig. (16) where it is observed that at low r, a scaling corresponding to r^2 is observed. This is in accordance with findings in Grossmann and Mertens (1992). At larger values of r, the r^2 scaling transitions to a $r^{4/3}$ scaling at relatively higher compressibility (i.e. $\alpha = 1.0$) and r scaling at $\alpha = 0.25$. Eventually, it is expected that an $r^{2/3}$ behavior must emerge with perfect incompressibility. The aforementioned observations hold true for both longitudinal and transverse second-order structure functions. Fig. (17) shows the third-order velocity structure functions for the longitudinal and transverse directions for the 2D test case. One can observe an inertial range scaling that follows $r^{4/3}$ for higher α while gradually decreasing in steepness to a r scaling for the longitudinal direction. In contrast, the transverse third-order structure function appears to show a r^2 scaling at higher values of α with r scaling corresponding to lower α and weaker compressibility. It can be observed that the velocity-structure functions for three-dimensional simulations generally obey K41 predictions (for lower values of α indicating weak compressibility) as against their two-dimensional counterparts.

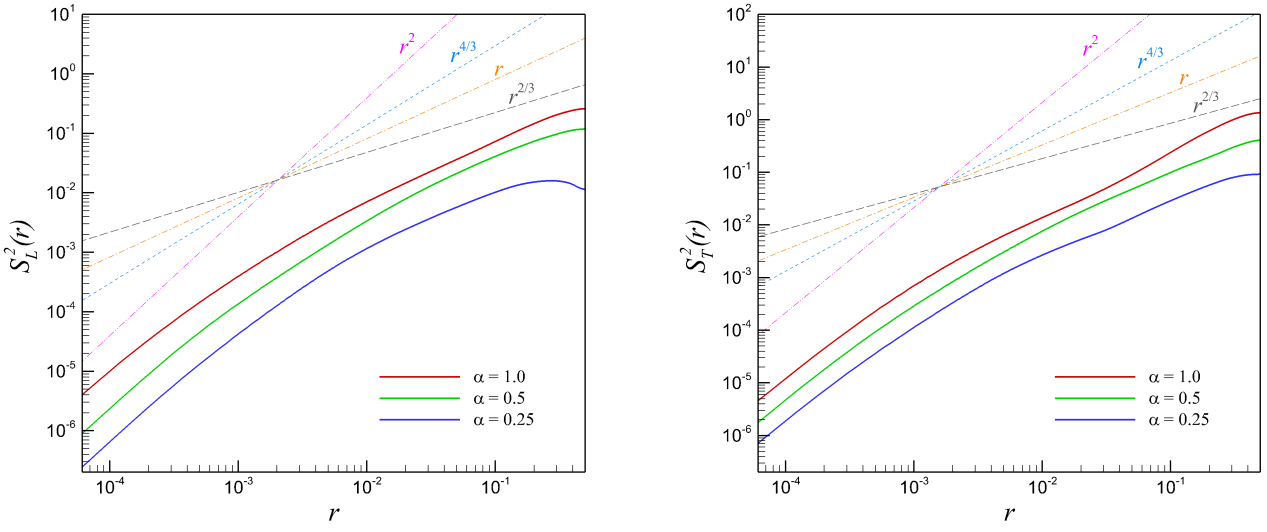

Figure 16. Second-order velocity structure functions for the 2D KHI turbulence. Left: longitudinal ($\boldsymbol{u} \parallel \boldsymbol{r}$). Right: transverse ($\boldsymbol{u} \perp \boldsymbol{r}$).

4 Conclusions

In this investigation, data from high-fidelity numerical experiments are utilized to study scaling behavior for statistical quantities such as spectra and structure functions. We study two test cases given by the Kelvin-Helmholtz instability problem in two and three dimensions to simulate the effect of high aspect ratios on spectral scaling laws and structure functions. Our spectra are given by the averaged kinetic energy magnitude and the averaged density-weighted kinetic energy magnitude and it is observed that while both quantities exhibit similar trends in three dimensions, the density-weighted kinetic energy spectra shows varying

Nonlin. Processes Geophys. Discuss., https://doi.org/10.5194/npg-2017-67
Manuscript under review for journal Nonlin. Processes Geophys.
Discussion started: 12 February 2018

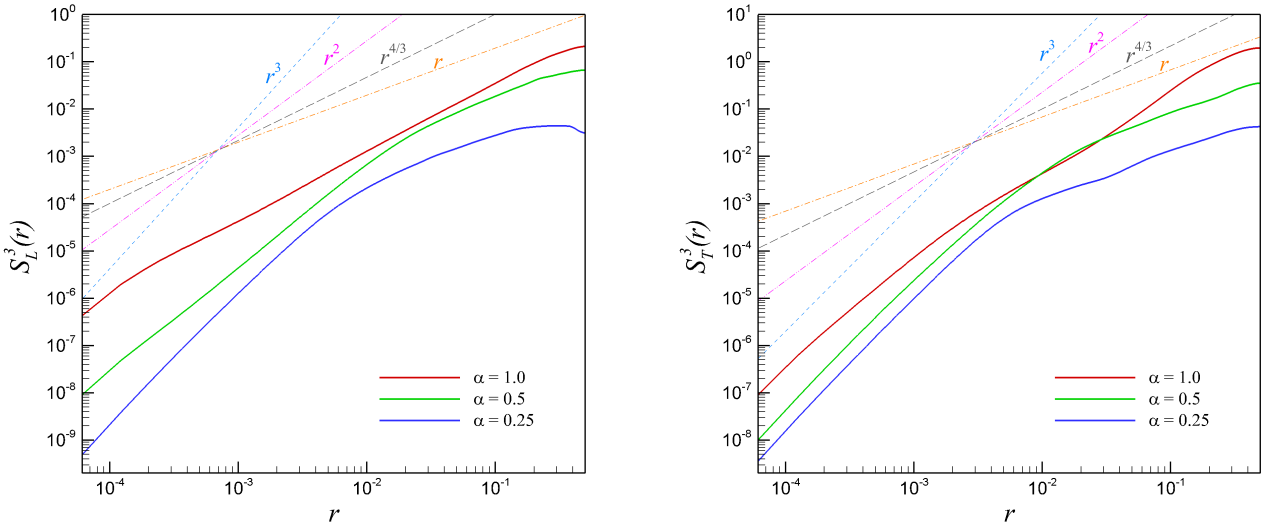

Figure 17. Third-order velocity structure functions for the 2D KHI turbulence. Left: longitudinal ($\boldsymbol{u} \parallel \boldsymbol{r}$). Right: transverse ($\boldsymbol{u} \perp \boldsymbol{r}$).

scaling tendencies in two dimensions when high compressibility situations are studied. This is demonstrated by a flattening of the density-weighted energy spectra, expected to exhibit k^{-3} scaling in the incompressible limit, to $k^{-7/3}$ scaling for higher compressibility. Variations are also seen in the scaling of the dissipation range. This prompts us to investigate the density power spectrum for both two and three-dimensional cases and it is observed that two distinct inertial and dissipation range behavior can be observed. The three-dimensional case shows a five-thirds scaling behavior in the inertial range with a k^{-6} scaling in the dissipation range. On the other hand, the two-dimensional case shows a $k^{-1/4}$ scaling in the inertial range with a k^{-3} scaling in the dissipation range. This basically demonstrates that an extremely high aspect ratio fundamentally alters the spectral content of density in flows exhibiting compressibility and stratification. Our two-point structure functions in the three-dimensional test case conform with predictions from K41 theory for second and third orders when the cases with lowest shearing velocities are examined (corresponding to weak compressibility). Two-dimensional structure functions are also plotted for the purpose of discerning the differences with the three-dimensional test case. It is observed that increased compressibility leads to a steeper scaling (as seen for both second and third order structure functions) for the two-dimensional test case. The scaling behavior exhibited by the density power spectrum for the two-dimensional test, combined with the trends observed in the structure functions indicate that nonlinear processes exhibiting extreme aspect ratios may have a fundamentally different set of nonlinear interactions as compared to moderate aspect ratios (which may be classified as three-dimensional). Incorporating the effect of boundary conditions, which inevitably lead to large scale anisotropy (recall the inverse energy cascade in 2D flows) into the scaling tendencies exhibited here would account for further interesting deviations from 3D counterparts. This remains a topic of focus for future investigation.

Nonlin. Processes Geophys. Discuss., https://doi.org/10.5194/npg-2017-67
Manuscript under review for journal Nonlin. Processes Geophys.
Discussion started: 12 February 2018

Acknowledgements. All numerical experiments have been performed using the resources of the Oklahoma State University High Performance Computing facilities.

References

Aluie, H.: Scale decomposition in compressible turbulence, Physica D, 247, 54–65, 2013.

Banerjee, S. and Galtier, S.: Exact relation with two-point correlation functions and phenomenological approach for compressible magneto-hydrodynamic turbulence, Phys. Rev. E, 87, 013 019, 2013.

Batchelor, G. K.: Computation of the Energy Spectrum in Homogeneous Two-Dimensional Turbulence, Phys. Fluids, 12, 233, 1969.

Bershadskii, A.: Distributed chaos and inertial ranges in turbulence, arXiv preprint arXiv:1609.01617, 2016.

Biskamp, D. and Schwarz, E.: On two-dimensional magnetohydrodynamic turbulence, Phys. Plasmas, 8, 3282–3292, 2001.

Blaisdell, G. A., Mansour, N. N., and Reynolds, W. C.: Compressibility effects on the growth and structure of homogeneous turbulent shear flow, J. Fluid Mech., 256, 443–485, 1993.

Boffetta, G. and Ecke, R. E.: Two-dimensional turbulence, Annu Rev. Fluid Mech., 44, 427–451, 2012.

Boffetta, G. and Mazzino, A.: Incompressible Rayleigh-Taylor Turbulence, Annu. Rev. Fluid. Mech., 49, 119–143, 2017.

Bos, W. J. and Bertoglio, J. P.: Dynamics of spectrally truncated inviscid turbulence, Phys. Fluids, 18, 071 701, 2006.

Clercx, H. J. H. and van Heijst, G. J. F.: Dissipation of coherent structures in confined two-dimensional turbulence, Phys. Fluids, 29, 111 103, 2017.

Domaradzki, J. A. and Carati, D.: An analysis of the energy transfer and the locality of nonlinear interactions in turbulence, Phys. Fluids, 19, 085 112, 2007.

Falceta-Goncalves, D., Kowal, G., Falgarone, E., and Chian, A.: Turbulence in the interstellar medium, Nonlinear Proc. Geoph., 21, 587–604, 2014.

Goldreich, P. and Sridhar, S.: Magnetohydrodynamic turbulence revisited, Astrophys. J., 485, 680, 1997.

Grossmann, S. and Mertens, P.: Structure functions in two-dimensional turbulence, Z. Phy. B. Con. Mat., 88, 105–116, 1992.

Hopfinger, E. J.: Turbulence in stratified fluids: A review, J. Geophys. Res.-Oceans, 92, 5287–5303, 1987.

Hwang, K., Goldstein, M. L., Kuznetsova, M. M., Wang, Y., Viñas, A. F., and Sibeck, D. G.: The first in situ observation of Kelvin-Helmholtz waves at high-latitude magnetopause during strongly dawnward interplanetary magnetic field conditions, J. Geophys. Res.-Space, 117, 2012.

Iroshnikov, P. S.: Turbulence of a conducting fluid in a strong magnetic field, Sov. Astron., 7, 566, 1964.

Kadomtsev, B. B. and Petviashvili, V. I.: Acoustic turbulence, in: Sov. Phys. Dokl., vol. 18, p. 115, 1973.

Kida, S. and Orszag, S. A.: Energy and spectral dynamics in forced compressible turbulence, J. Sci. Comput., 5, 85–125, 1990.

Kida, S., Murakami, Y., Ohkitani, K., and Yamada, M.: Energy and flatness spectra in a forced turbulence, J. Phys. Soc. Jpn, 59, 4323–4330, 1990.

Kolmogorov, A. N.: The local structure of turbulence in incompressible viscous fluid for very large Reynolds numbers, in: Dokl. Akad. Nauk SSSR, vol. 30, pp. 299–303, 1941.

Kraichnan, R. H.: Inertial-range spectrum of hydromagnetic turbulence, Phys. Fluids, 8, 1385–1387, 1965.

Kraichnan, R. H.: Inertial ranges in two-dimensional turbulence, The Phys. Fluids, 10, 1417–1423, 1967.

Kritsuk, A. G., Norman, M. L., Padoan, P., and Wagner, R.: The statistics of supersonic isothermal turbulence, Astrophys. J., 665, 416, 2007.

Kuznetsov, E. A. and Sereshchenko, E. V.: Anisotropic characteristics of the Kraichnan direct cascade in two-dimensional hydrodynamic turbulence, JETP Lett+, 102, 760–765, 2015.

Leith, C. E.: Atmospheric predictability and two-dimensional turbulence, J. Atmos. Sci., 28, 145–161, 1971.

Lele, S. K.: Compressibility effects on turbulence, Annu. Rev. Fluid Mech., 26, 211–254, 1994.

Mac Low, M. and Klessen, R. S.: Control of star formation by supersonic turbulence, Rev. Mod. Phys., 76, 125, 2004.

Mac Low, M., Klessen, R. S., Burkert, A., and Smith, M. D.: Kinetic energy decay rates of supersonic and super-Alfvénic turbulence in star-forming clouds, Phys. Rev. Lett., 80, 2754, 1998.

Maulik, R. and San, O.: Resolution and energy dissipation characteristics of implicit LES and explicit filtering models for compressible turbulence, Fluids, 2, 14, 2017.

Moin, A. S. and Yaglom, A. M.: Statistical fluid mechanics, Vol. 2, 1975.

Moura, R. C., Mengaldo, G., Peiró, J., and Sherwin, S. J.: On the eddy-resolving capability of high-order discontinuous Galerkin approaches to implicit LES/under-resolved DNS of Euler turbulence, J. Comput. Phys., 330, 615–623, 2017.

Ottaviani, M.: Scaling laws of test particle transport in two-dimensional turbulence, Europhys. Lett., 20, 111, 1992.

Padoan, P. and Nordlund, Å.: The stellar initial mass function from turbulent fragmentation, Astrophys. J., 576, 870, 2002.

Passot, T., Pouquet, A., and Woodward, P.: The plausibility of Kolmogorov-type spectra in molecular clouds, Astron. Astrophys., 197, 228–234, 1988.

Peltier, W. R. and Caulfield, C. P.: Mixing efficiency in stratified shear flows, Annu. Rev. Fluid Mech., 35, 135–167, 2003.

Qiu, X., Ding, L., Huang, Y., Chen, M., Lu, Z., Liu, Y., Zhou, Q., et al.: Intermittency measurement in two-dimensional bacterial turbulence, Phys. Rev. E, 93, 062 226, 2016.

Roe, P. L.: Approximate Riemann solvers, parameter vectors, and difference schemes, J. Comput. Phys., 43, 357–372, 1981.

Shivamoggi, B. K.: Spectral laws for the compressible isotropic turbulence, Phys. Lett. A, 166, 243–248, 1992.

Shivamoggi, B. K.: Spatial intermittency in the classical two-dimensional and geostrophic turbulence, Ann. Phys.-New York, 270, 263–291, 1998.

Shivamoggi, B. K.: Magnetohydrodynamic turbulence: Generalized formulation and extension to compressible cases, Ann. Phys.-New York, 323, 1295–1303, 2008.

Shivamoggi, B. K.: Compressible turbulence: Multi-fractal scaling in the transition to the dissipative regime, Physica A, 390, 1534–1538, 2011.

Shivamoggi, B. K.: Singularities in fully developed turbulence, Phys. Lett. A, 379, 1887–1892, 2015.

Sun, B.: The temporal scaling laws of compressible turbulence, Mod. Phys. Lett. B, 30, 1650 297, 2016.

Sytine, I. V., Porter, D. H., Woodward, P. R., Hodson, S. W., and Winkler, K.: Convergence tests for the piecewise parabolic method and Navier-Stokes solutions for homogeneous compressible turbulence, J. Comput. Phys., 158, 225–238, 2000.

Thomson, W.: Hydrokinetic solutions and observations, Philos. Mag., 42, 362–377, 1871.

Vassilicos, J. C.: Dissipation in turbulent flows, Annu. Rev. Fluid Mech., 47, 95–114, 2015.

Wang, J., Yang, Y., Shi, Y., Xiao, Z., He, X. T., and Chen, S.: Cascade of kinetic energy in three-dimensional compressible turbulence, Phys. Rev. Lett., 110, 214 505, 2013.

Werne, J. and Fritts, D. C.: Stratified shear turbulence: Evolution and statistics, Geophys. Res. Lett., 26, 439–442, 1999.

Westernacher-Schneider, J. R., Lehner, L., and Oz, Y.: Scaling relations in two-dimensional relativistic hydrodynamic turbulence, J. High. Energy Phys., 2015, 1–31, 2015.

Zhou, Y., Grinstein, F. F., Wachtor, A. J., and Haines, B. M.: Estimating the effective Reynolds number in implicit large-eddy simulation, Phys. Rev. E, 89, 013 303, 2014.